Electronic Supplementary Material (ESI) for Physical Chemistry Chemical Physics.

Electronic Supplementary Information for "Characterization of the Temperature and Humidity-Dependent Phase Diagram of Amorphous Nanoscale Organic Aerosols"

Nicholas E. Rothfuss[a] and Markus D. Petters[a]

a Department of Marine, Earth, and Atmospheric Sciences, North Carolina State University, Raleigh, NC, USA 26795. Email: mdpetter@ncsu.edu

Contents

Abbreviations used in this document: temperature (*T*), viscosity (*η*), coalescence characteristic relative humidity (RH_r), coalescence characteristic temperature (T_r), uncoalesced dimer diameter (D_{uc}), coalesced dimer diameter (D_c), logistic curve steepness parameter (*k*), glass transition temperature (T_g), mass-based hygroscopicity parameter (κ_m)

1. Additional Figures Referenced in the Manuscript

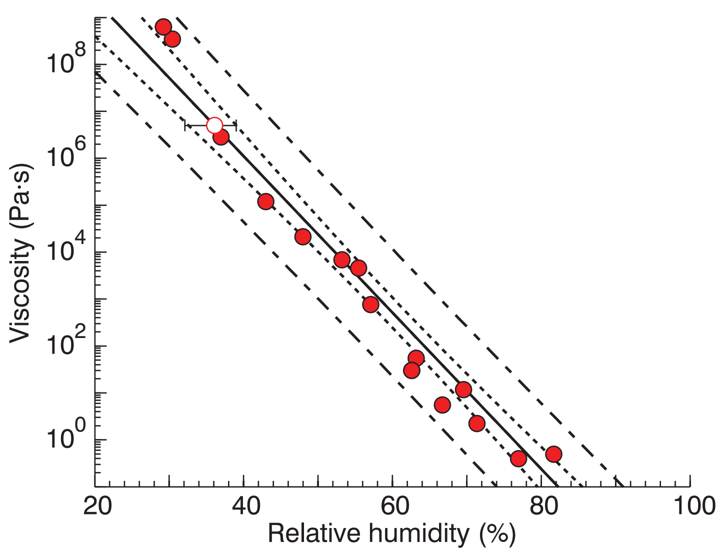

Figure S1. Plot depicting how the relative humidity where viscosity equals 5 x 10^6 Pa s (open red circle) was interpolated from data digitized from Power et al.[1] (solid red circles). Solid black line: fitted linear regression line; dotted black lines: 95% confidence interval of the fitted regression line; dashed black lines: 95% observational prediction interval of the fitted regression line.

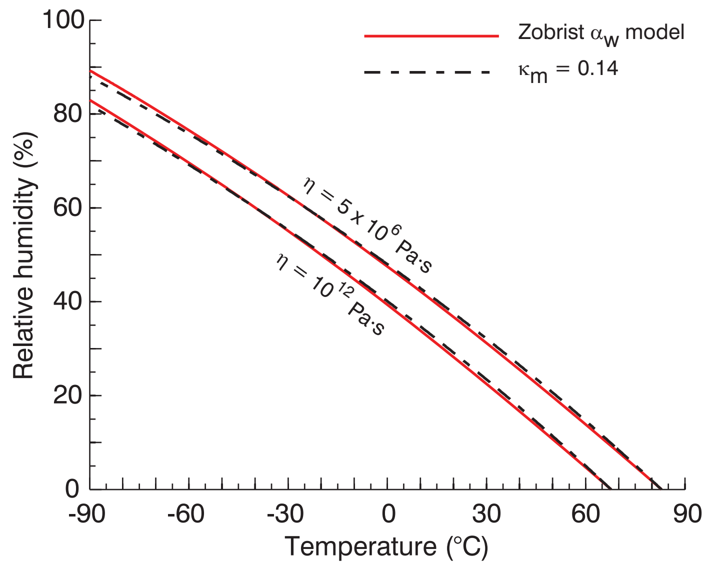

Figure S2. Variation in placement of modelled 5x10^6 Pa·s and 10^{12} Pa·s isopleths where the relationship between sucrose mass fraction and water activity was modelled using either the approach of Zobrist et al.[2] or a mass-based hygroscopicity parameter approach[3] with a fixed parameter value of 0.14, characteristic of sucrose.

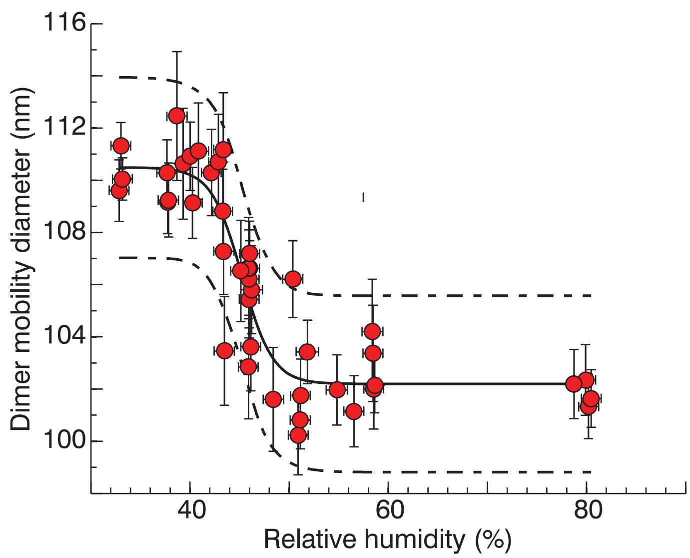

Figure S3. Measurements of dimer mobility diameter versus RH for the sucrose-sucrose isothermal humidification experiment performed at T = 4 °C, including fitted logistic curve (solid black curve) and 95% observational prediction interval (dashed black curves). (RH_r = 45.2% ± 1.0%, D_{uc} = 110.5 nm ± 1.2 nm, D_c = 102.2 nm ± 0.9 nm, k = 0.6430)

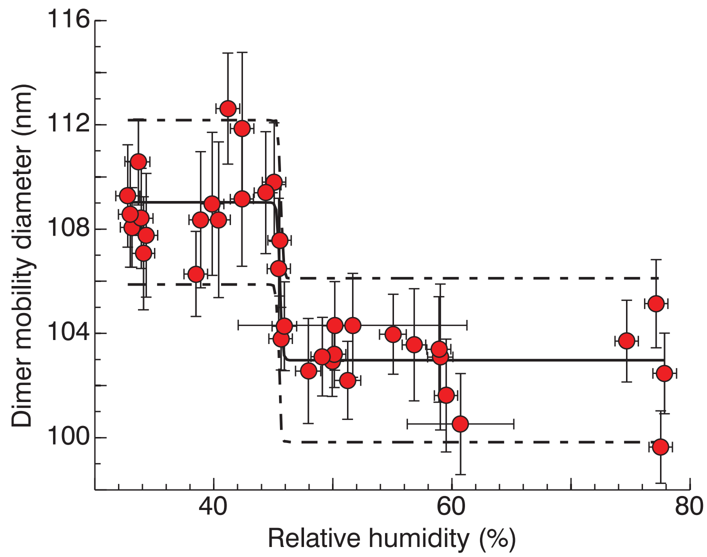

Figure S4. Measurements of dimer mobility diameter versus RH for the sucrose-sucrose isothermal humidification experiment performed at T = 5 °C, including fitted logistic curve (solid black curve) and 95% observational prediction interval (dashed black curves). (RH_r = 45.5% ± 0.1%, D_{uc} = 109.0 nm ± 0.8 nm, D_c = 103.0 nm ± 0.7 nm, k = 9.525)

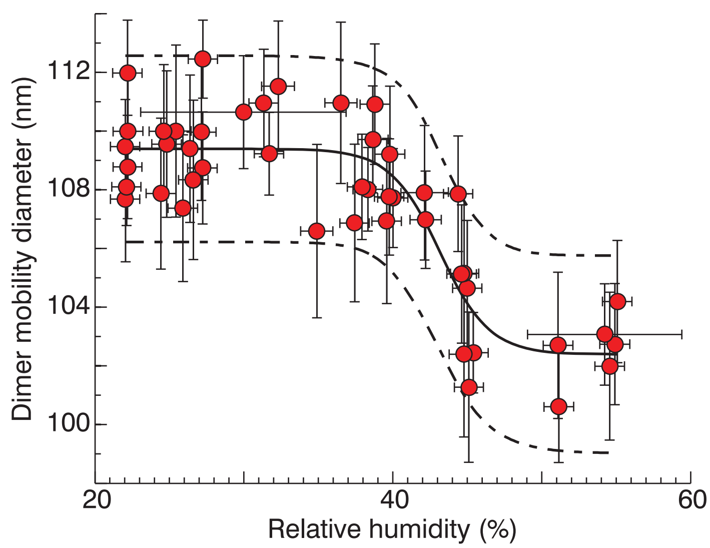

Figure S5. Measurements of dimer mobility diameter versus RH for the sucrose-sucrose isothermal humidification experiment performed at T = 12 °C, including fitted logistic curve (solid black curve) and 95% observational prediction interval (dashed black curves). (RH_r = 43.2% ± 1.5%, D_{uc} = 109.4 nm ± 0.7 nm, D_c = 102.4 ± 1.3 nm, k = 0.5982)

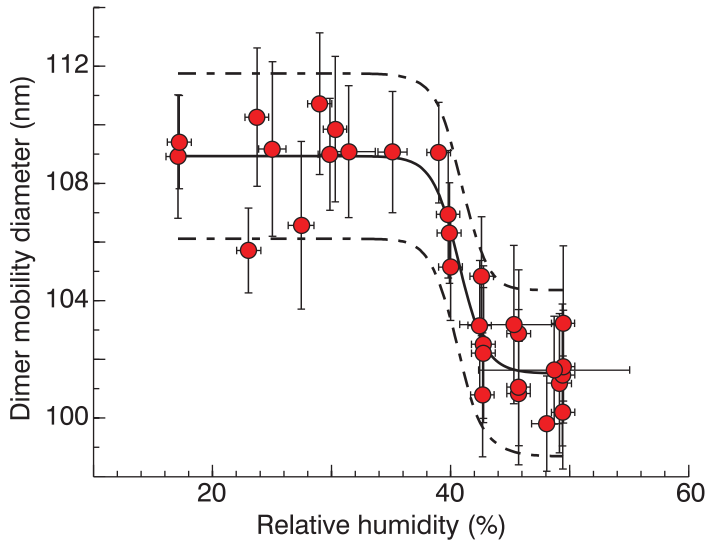

Figure S6. Measurements of dimer mobility diameter versus RH for the sucrose-sucrose isothermal humidification experiment performed at T = 15 °C, including fitted logistic curve (solid black curve) and 95% observational prediction interval (dashed black curves). (RH_r = 40.7% ± 1.0%, D_{uc} = 108.9 nm ± 0.8 nm, D_c = 101.5 nm ± 0.9 nm, k = 0.8967)

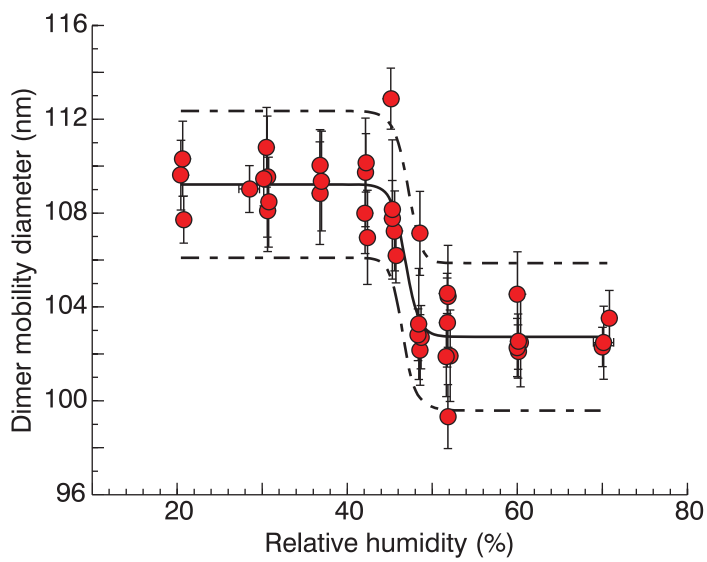

Figure S7. Measurements of dimer mobility diameter versus RH for the sucrose-sucrose cooling cycle experiment performed new for this work, including fitted logistic curve (solid black curve) and 95% observational prediction interval (dashed black curves). (RH_r = 46.8% ± 1.2%, T_r = 0.1 °C ± 1.2 °C, D_{uc} = 109.2 nm ± 0.8 nm, D_c = 102.7 ± 0.8 nm, k = 1.222)

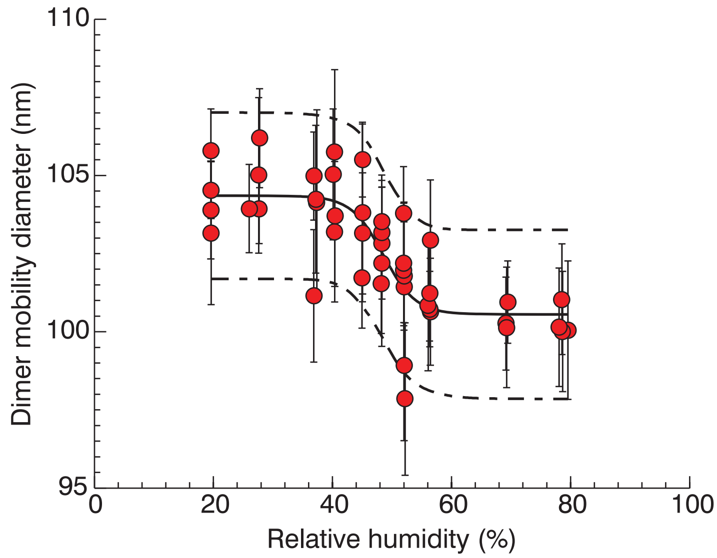

Figure S8. Measurements of dimer mobility diameter versus RH for the first sucrose-SDS cooling cycle experiment referenced in Table 1 of the manuscript, including fitted logistic curve (solid black curve) and 95% observational prediction interval (dashed black curves). (RH_r = 48.6% ± 3.1%, T_r = -1.3 °C ± 1.1 °C, D_{uc} = 104.4 nm ± 0.7 nm, D_c = 100.6 nm ± 0.9 nm, k = 0.3698)

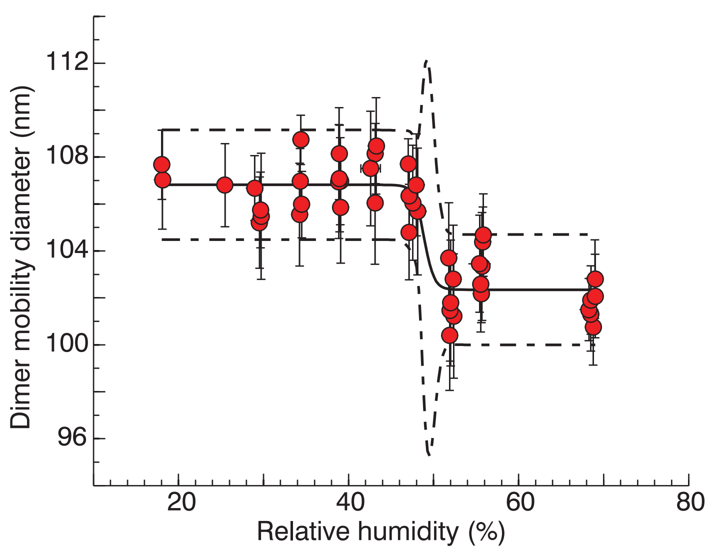

Figure S9. Measurements of dimer mobility diameter versus RH for the second sucrose-SDS cooling cycle experiment referenced in Table 1 of the manuscript, including fitted logistic curve (solid black curve) and 95% observational prediction interval (dashed black curves). (RH_r = 48.9% ± 3.5%, T_r = -3.4 °C, D_{uc} = 106.8 nm ± 0.5 nm, D_c = 102.3 nm ± 0.6 nm, k = 1.697)

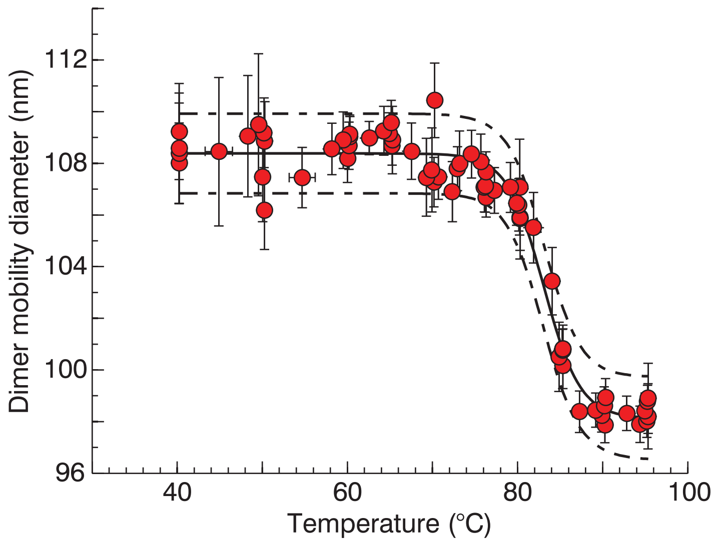

Figure S10. Measurements of dimer mobility diameter versus RH for the first sucrose-sucrose heating cycle experiment referenced in Table 1 of the manuscript, including fitted logistic curve (solid black curve) and 95% observational prediction interval (dashed black curves). (T_r = 83.1 °C ± 0.6 °C), RH_r = 0.8% ± 0.1%, D_{uc} = 108.4 nm ± 0.3 nm, D_c = 98.1 nm ± 0.5 nm, k = 0.4646)

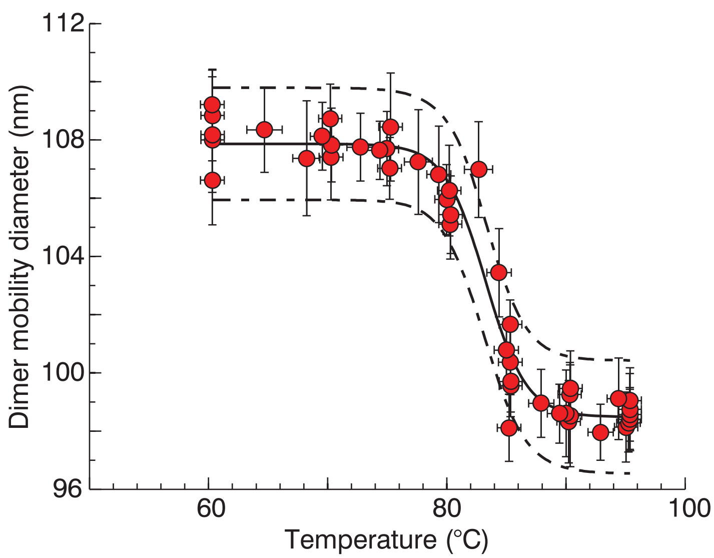

Figure S11. Measurements of dimer mobility diameter versus RH for the second sucrose-sucrose heating cycle experiment referenced in Table 1 of the manuscript, including fitted logistic curve (solid black curve) and 95% observational prediction interval (dashed black curves). (T_r = 83.2 °C ± 0.7 °C, RH_r = 0.8% ± 0.1%, D_c = 107.9 nm ± 0.5 nm, D_{uc} = 98.5 nm ± 0.5 nm, k = 0.5814).

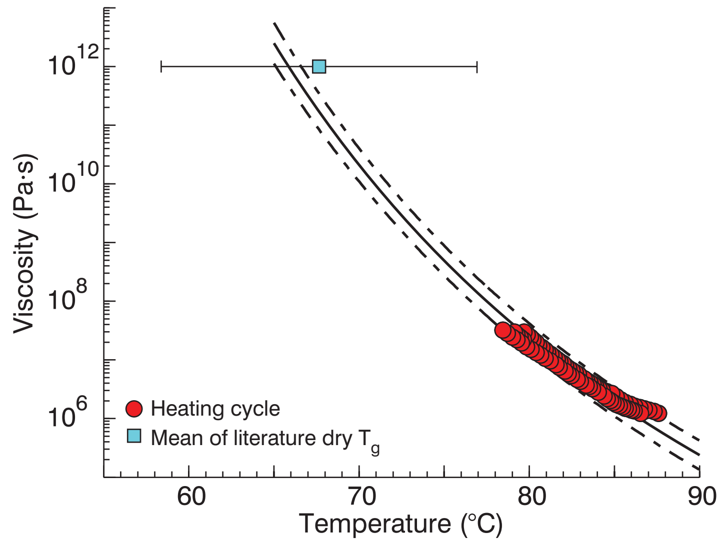

Figure S12. Fitted VFT curve as derived for sucrose when fixing the *A* parameter to a value of -5. The curve fit utilized both viscosity data derived from heating cycle experiments and mean literature T_g. Error bars associated with the glass transition point correspond to one standard deviation of the literature values utilized. Black dashed curves correspond to the 95% observational prediction interval of the fitted VFT equation.

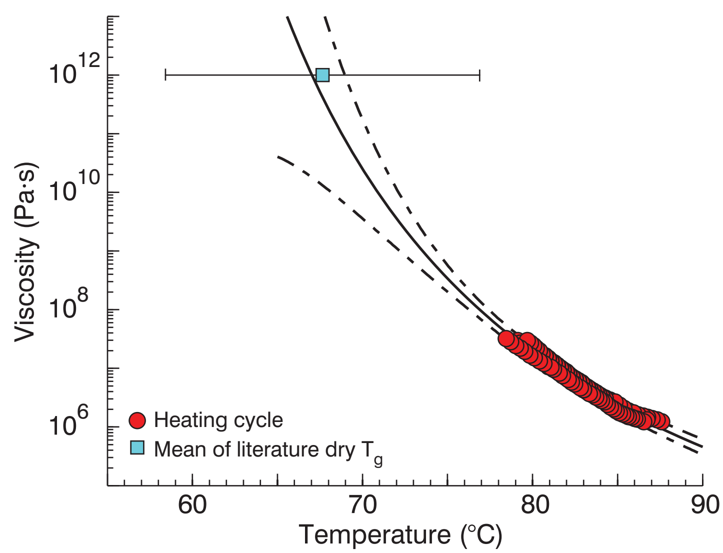

Figure S13. Fitted VFT curve as derived for sucrose utilizing only data from heating cycle experiments and not considering mean literature T_g. Error bars associated with the glass transition point correspond to one standard deviation of the literature values utilized. Black dashed curves correspond to the 95% observational prediction interval of the fitted VFT equation.

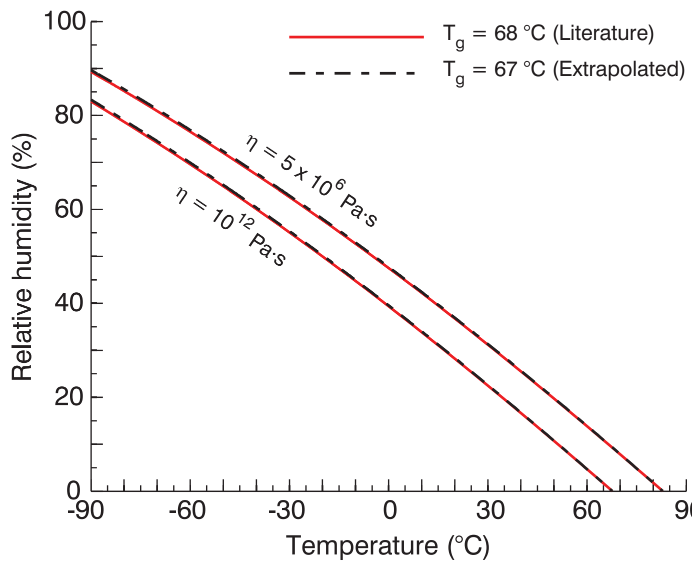

Figure S14. Variation in placement of modelled 5x10^6 Pa·s and 10^{12} Pa·s isopleths where dry sucrose glass transition temperature was determined either using an average literature value or via extrapolation of our own dry sucrose viscosity measurements.

2. Additional Table Referenced in the Manuscript

Table S1. Viscosity measurements for amorphous sucrose at various temperatures as derived from the three heating cycle experiments performed for this work. Experiment numbering corresponds to order of mention in Table 1 of the main manuscript.

Experiment #1 (T_r = 83.1 °C)		Experiment #2 (T_r = 83.2 °C)		Experiment #3 (T_r = 82.8 °C)	
T (°C)	η (Pa·s)	T (°C)	η (Pa·s)	T (°C)	η (Pa·s)
78.46	3.22 X 10^7	79.69	2.96 X 10^7	79.13	2.96 X 10^7
78.73	2.82 X 10^7	79.87	2.66 X 10^7	79.30	2.66 X 10^7
79.01	2.47 X 10^7	80.05	2.41 X 10^7	79.48	2.42 X 10^7
79.29	2.18 X 10^7	80.22	2.18 X 10^7	79.66	2.19 X 10^7
79.56	1.92 X 10^7	80.4	1.97 X 10^7	79.83	1.99 X 10^7
79.84	1.69 X 10^7	80.58	1.77 X 10^7	80.01	1.80 X 10^7
80.12	1.52 X 10^7	80.75	1.62 X 10^7	80.18	1.64 X 10^7
80.39	1.35 X 10^7	80.93	1.48 X 10^7	80.36	1.51 X 10^7
80.67	1.20 X 10^7	81.10	1.35 X 10^7	80.54	1.38 X 10^7
80.95	1.07 X 10^7	81.28	1.23 X 10^7	80.71	1.26 X 10^7
81.23	9.61 X 10^6	81.46	1.12 X 10^7	80.89	1.15 X 10^7
81.50	8.66 X 10^6	81.63	1.02 X 10^7	81.07	1.05 X 10^7
81.78	7.69 X 10^6	81.81	9.43 X 10^6	81.24	9.72 X 10^6
82.06	6.92 X 10^6	81.99	8.68 X 10^6	81.42	8.98 X 10^6
82.33	6.23 X 10^6	82.16	7.89 X 10^6	81.59	8.22 X 10^6
82.61	5.60 X 10^6	82.34	7.22 X 10^6	81.77	7.50 X 10^6
82.89	5.05 X 10^6	82.51	6.67 X 10^6	81.95	6.94 X 10^6
83.16	4.55 X 10^6	82.69	6.12 X 10^6	82.12	6.41 X 10^6
83.44	4.12 X 10^6	82.87	5.62 X 10^6	82.30	5.88 X 10^6
83.72	3.77 X 10^6	83.04	5.18 X 10^6	82.48	5.43 X 10^6
83.99	3.45 X 10^6	83.22	4.76 X 10^6	82.65	5.01 X 10^6
84.27	3.13 X 10^6	83.39	4.39 X 10^6	82.83	4.63 X 10^6
84.55	2.87 X 10^6	83.57	4.07 X 10^6	83.01	4.28 X 10^6
84.83	2.65 X 10^6	83.75	3.78 X 10^6	83.18	3.98 X 10^6
85.10	2.34 X 10^6	83.92	3.54 X 10^6	83.36	3.72 X 10^6
85.38	2.09 X 10^6	84.10	3.27 X 10^6	83.53	3.48 X 10^6
85.66	1.90 X 10^6	84.28	3.04 X 10^6	83.71	3.23 X 10^6
85.93	1.74 X 10^6	84.45	2.83 X 10^6	83.89	3.00 X 10^6
86.21	1.62 X 10^6	84.63	2.66 X 10^6	84.06	2.81 X 10^6
86.49	1.52 X 10^6	84.80	2.42 X 10^6	84.24	2.65 X 10^6
86.76	1.45 X 10^6	84.98	2.21 X 10^6	84.42	2.41 X 10^6
87.04	1.38 X 10^6	85.16	2.03 X 10^6	84.59	2.20 X 10^6
87.32	1.33 X 10^6	85.33	1.88 X 10^6	84.77	2.03 X 10^6
87.59	1.22 X 10^6	85.51	1.76 X 10^6	84.94	1.88 X 10^6
		85.69	1.65 X 10^6	85.12	1.76 X 10^6
		85.86	1.57 X 10^6	85.30	1.66 X 10^6
		86.04	1.50 X 10^6	85.47	1.58 X 10^6
		86.21	1.44 X 10^6	85.65	1.51 X 10^6
		86.39	1.39 X 10^6	85.83	1.45 X 10^6
		86.57	1.35 X 10^6	86.00	1.40 X 10^6
		86.74	1.31 X 10^6	86.18	1.36 X 10^6
				86.35	1.32 X 10^6
				86.53	1.22 X 10^6

3. References

1 R. M. Power, S. H. Simpson, J. P. Reid and A. J. Hudson, *Chem. Sci.*, 2013, **4**, 2597–2604.

2 B. Zobrist, C. Marcolli, D. A. Pedernera and T. Koop, *Atmos. Chem. Phys.*, 2008, **8**, 5221–5244.

3 E. Mikhailov, S. Vlasenko, D. Rose and U. Pöschl, *Atmos. Chem. Phys.*, 2013, **13**, 717–740.